ISSN 0208-7774 TRIBOLOGIA 3/2018 p. 69–76

Waldemar KOSZELA[*], Lidia GAŁDA[*], Andrzej DZIERWA[*], Pawel PAWLUS[*], Jarosław SĘP[*], Sławomir OCHWAT[**]

THE EFFECT OF SURFACE TEXTURING ON THE FRICTIONAL RESISTANCE OF STEEL-BRONZE ASSEMBLY IN LUBRICATED SLIDING

WPŁYW TEKSTUROWANIA POWIERZCHNI NA OPORY TARCIA UKŁADU STAL–BRĄZ W WARUNKACH SMAROWANIA

Key words: surface texturing, oil pockets, burnishing, steel-bronze assembly, coefficient of friction.

Abstract

The experiments were carried out using a block-on-ring tester. The block samples made from bronze CuSn10P of 138 HB hardness were burnished to obtain surfaces with circular oil pockets. Rings were made from 42CrMo4 steel of hardness 40 HRC. Friction tests were conducted at a constant normal load of 900 N. Tests were carried out at increasing sliding speeds of the range 0.08 – 0.82 m/s, starting from the lowest speed. The every speed was maintained for two minutes. The tested assembly was inserted in the reservoir of mineral oil L-AN 46.

It was found that the dimple presence on block surface reduced the friction coefficient substantially compared to non-textured turned surfaces. The area density of dimples smaller than 15% (particularly 4.5% and 6%) was beneficial.

Słowa kluczowe: teksturowanie powierzchni, kieszenie olejowe, nagniatanie, skojarzenie materiałowe stal-brąz, współczynnik tarcia.

Streszczenie

Przeprowadzono badania tribologiczne w układzie rolka-klocek. Powierzchnie klocka (wycinka pierścienia) z brązu CuSn10P o twardości 138 HB zawierały sferyczne kieszenie smarowe uzyskane metodą wygniatania. Rolki wykonano ze stali 42CrMo4 o twardości 40 HRC. Badania tribologiczne przeprowadzono przy stałym obciążeniu normalnym wynoszącym 900 N i zwiększającej się prędkości ślizgania w zakresie 0,08–0,82 m/s, utrzymywanej w czasie dwóch minut. Skojarzenie trące smarowano olejem L-AN 46 znajdującym się w zbiorniku.

Stwierdzono, że teksturowanie powierzchni klocka spowodowało istotne zmniejszenie oporów tarcia w porównaniu z parą cierną zawierającą gładkie powierzchnie, szczególnie przy niewielkich stopniach pokrycia wgłębieniami (4,5 i 6%).

INTRODUCTION

Surface texturing has attracted attention of tribologists, since it can be used to improve the tribological properties of sliding elements without changing materials and lubricants. Oil pockets (micropits, holes, dimples, or cavities) may reduce friction acting as micro-hydrodynamic bearings and/or as reservoirs of lubricant. Various techniques can be used for surface texturing including honing **[L. 1, 2]**, ion beam texturing, abrasive jet machining **[L. 3, 4]** etching techniques, laser texturing **[L. 5, 6]**, burnishing **[L. 7, 8]**, or combination of these methods **[L. 9, 10]**.

Stribeck showed that friction for sliding bearings started at high friction at low speeds, decreased to a minimum friction and then again increased at higher speeds. Different regions of the "Stribeck curve" are associated with different lubrication regimes. The Stribeck curve is of particular use in determining the type of lubrication. Because the lubricant has a very

[*] Rzeszow University of Technology, Faculty of Mechanical Engineering and Aeronautics, Powstancow Warszawy 8, 35-959 Rzeszow, Poland.

[**] AEROGEARBOX INTL., Przemysłowa 3 street, 39-100 Ropczyce, Poland.

strong influence on the friction, the Stribeck curve maps the relationship of the coefficient of friction between two sliding bodies separated by the fluid layer to the Hersey number $v\eta/p$, which is dependent on the applied pressure p, relative velocity between sliding elements v, and the lubricant viscosity η **[L. 11, 12]**. Researchers found that surface texturing of contacting elements reduced the friction force substantially in comparison to non-textured surfaces. Surface texturing was observed to expand the range of the hydrodynamic lubrication regime **[L. 7, 13, 14, 15, 16]**.

EXPERIMENTAL DETAILS

Friction tests were conducted with a block-on-ring machine in unidirectional sliding. The tribosystem consists of the stationary block (specimen) pressed at the required load Q against the ring (counter-specimen) rotating at the defined speed. The test was carried out under conformal contact conditions. The contact area was 100 mm^2. The construction of the friction rig allows measuring the friction force F between the ring and block by the force transducer. **Figure 1** shows a schematic diagram of the contact configuration. One can find a detailed description of this tester in **[L. 7]**. The block samples made from bronze CuSn10P of 138 HB hardness were burnished in order to obtain surfaces with circular oil pockets. Rings (rollers) were made from 42CrMo4 steel of hardness 40 HRC. Block shape and fixing in the tester T-05 were modified in order to improve intimate contact between sliding surfaces of block and roller. The block was cut out from a ring using the special instrumentation in order to obtain good repeatability for a high number of samples. In addition, correct co-acting between sliding elements was possible due to the machining of block and roller within desired tolerances, for the classic shape of the block and an increase in clearance difficulties in obtaining required adherence and conformal contact would be possible. Tests were conducted at increasing sliding speeds in the range of 0.08 – 0.82 m/s, starting from the smallest speed. Every speed was maintained for two minutes. The tested assembly was inserted in the reservoir (40 ml volume) of the lubricating fluid L-AN 46 (mineral oil, refined by anti-foaming, anti-oxidizing, and anti-corrosive agents). **Table 1** shows properties of this oil. Before each test, an assembly was subjected to a running--in of 5 min duration (ambient temperature, velocity 0.27 m/s, normal load 600 N). Friction tests were conducted at constant normal load of 900 N. In the beginning of each test, oil was heated to 60°C. During tests, the temperature of lubricant was continuously measured. The temperature sensor was located in the oil reservoir. Before the experiment, the viscosity of the oil at various temperatures was measured. Each friction experiment was repeated 3 times. In each repetition, different ring and block samples were used.

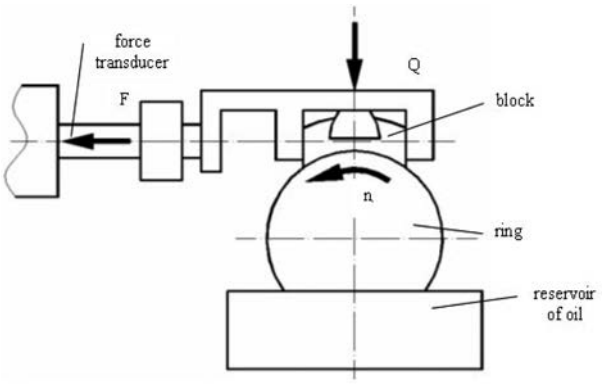

Fig. 1. The scheme of tested assembly
Rys. 1. Schemat badanego skojarzenia

Table 1. The parameters of L-AN 46 oil
Tabela 1. Właściwości oleju L-AN 46

Parameters	Units	Values
Kinematic viscosity in 40°C	mm^2/s	46.0
Kinematic viscosity in 100°C	mm^2/s	6.66
Viscosity index	-	96
Ignition temperature	°C	Min 170
Flow temperature	°C	Max -12
Density in 15°C	kg/m^3	880

A special tool acted as a hammer to form dimples on the block surfaces. The area densities of oil pockets Sp were from 4 to 20%, and they were selected based on initial research of the present authors and literature analysis **[L. 6, 9, 10]**. Block sample surfaces usually had dimples with depths of about 60 μm and diameters of about 1.2 mm. Only the depth and diameter of Sample 4 were smaller (45 μm and 1 mm, respectively). **Table 2** lists the characteristics of the tested block samples identified with the numbers 1–6. Sample 1, as the

reference element, was not burnished but precisely turned. Its surface roughness characterized by Ra parameter was 0.32 μm. Similar bronze specimens co-acted with steel rings in abrasive wear resistance tests **[L. 8]**.

Table 2. Characteristics of the tested bronze blocks
Tabela 2. Charakterystyka badanych próbek wykonanych z brązu

Block sample no.	1. turned	2.	3.	4.	5.	6.
Pit-area ratio S_p, %	–	4	6.5	10	15	20

Figure 2 shows the photos of the tested surfaces. In order to analyse changes in surface topography during friction tests, the measurements of block surface topographies were done using a white light interferometer (Talysurf CCI Lite) in the same places. The measurement area was 3.3 mm x 3.3 mm, sampling intervals were 3.2 μm in perpendicular directions, and the height resolution was 0.01 nm. Form was removed using polynomial of the 3rd degree, and digital filters were not used. The parameters from the ISO 25178 standard were calculated **[L. 17]**.

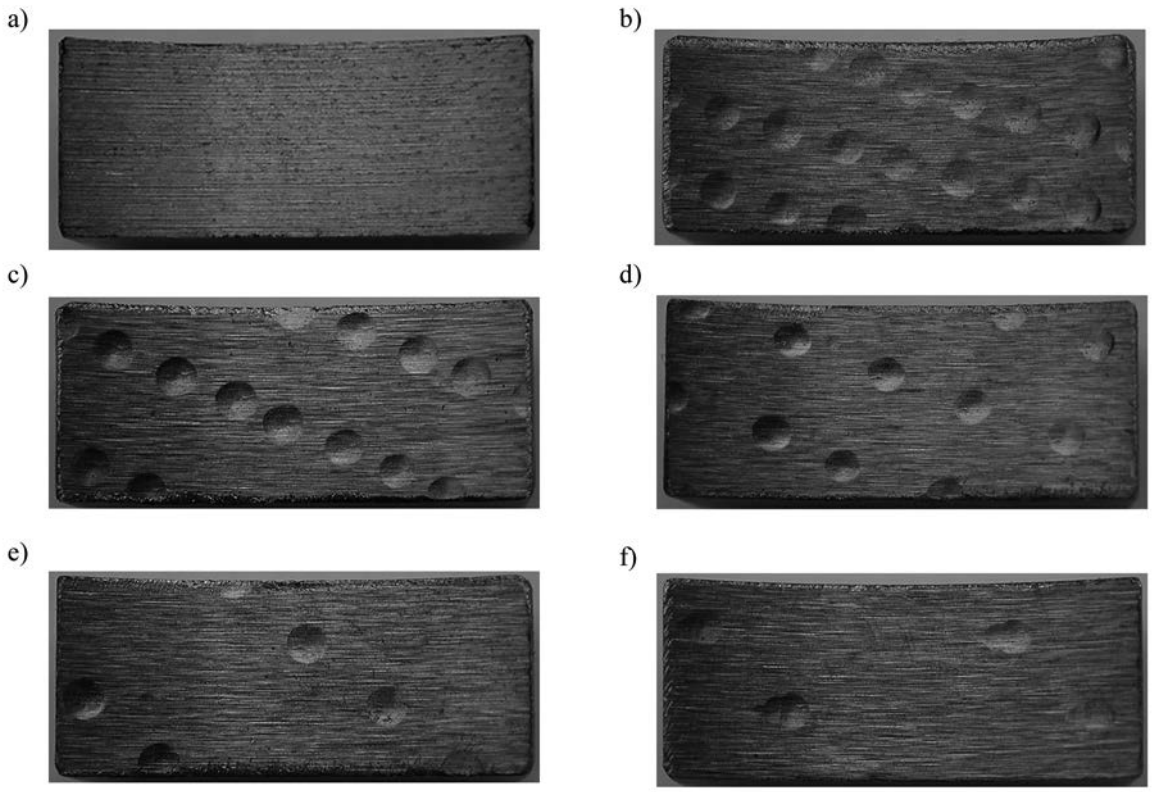

Fig. 2. Photos of block surfaces before tribologic tests: a) non-textured, b) Sp = 20%, c) Sp = 15%, d) Sp = 10%, e) Sp = 6.5%, f) Sp = 4%
Rys. 2. Fotografie próbek wykonanych z brązu przed rozpoczęciem badań: a) powierzchnia nieteksturowana, b) Sp = 20%, c) Sp = 15%, d) Sp = 10%, e) Sp = 6.5%, f) Sp = 4%

RESULTS AND DISCUSSION

The coefficient of friction μ was calculated as the ratio of friction force to normal force. **Figure 3** presents the dependence between sliding speed and the mean value of the coefficient of friction. **Table 3** presents the values of the relative scatter of the coefficient of friction for various sliding speeds. The relative scatter is defined as the ratio of the difference between maximum and minimum values of the coefficient of friction (due to test repetitions) to its average value.

Figure 4 shows example of friction coefficient variation versus λ parameter ($\lambda = v\eta/p$).

At low speeds, the coefficient of friction should be invariant with speed. This is the boundary lubrication region in which solid contact is the predominant mode of

friction. The region of the Stribeck curve at intermediate speeds, when coefficient of friction decreases with increasing speed, is the region of mixed lubrication.

In the region of fully developed hydrodynamic lubrication, at higher speeds, hydrodynamic pressure is sufficient to completely separate the sliding surfaces. In typical Stribeck curves, the coefficient of friction decreases as a function of velocity, and reaches a minimum and increases thereafter. However, in the work described in this paper, it was difficult to find the minimum of curves, especially for sliding pairs with block samples with dimple density S_p smaller than 15%, but similar shapes were found in other investigations **[L. 7, 11, 18]**.

Three different parts of curves shown **Figure 3** are visible. In the initial part, the friction force was almost constant when sliding speed increased up to 0.28 m/s. The coefficient of friction was usually between 0.1 and 0.16, and only for the sliding pair with specimen of the smallest pit-area ratio μ value, was it lower (0.08). In the second part, the coefficient of friction decreased for the sliding speed increasing from 0.28 m/s to 0.38 m/s for all the analysed cases. For higher speeds (the third part), the behaviours of sliding assemblies depended on the pit-area ratio of block samples. For area density smaller than 15%, the coefficient of friction decreased when sliding speed increased. For the highest speed, the coefficient of friction was lower than 0.02 for bronze samples with a dimple density of 4% and 6.5% and obtained a value of about 0.05 for sample with the pit-area ratio of 10%. For other assemblies, the friction force was stable or increased.

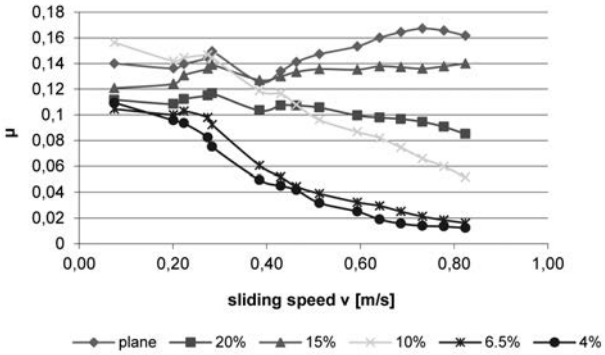

Fig. 3. Variation of the mean value of the coefficient of friction μ with sliding speed for assemblies with textured and non-textured surface

Rys. 3. Średnie wartości współczynnika tarcia μ w funkcji prędkości poślizgu dla skojarzeń ciernych zawierających powierzchnie teksturowane oraz nieteksturowane

Table 3. Relative scatters of the coefficient of friction, %
Tabela 3. Rozrzuty względne współczynnika tarcia, %

Sliding speed, m/s	Pit-area ratio S_p, %					
	-	4	6.5	10	15	20
0.08	14.1	19.5	28.5	6.5	33.2	12.1
0.2	6.2	5.2	18.3	14.3	24.5	13.5
0.22	14.3	7.5	33.2	14.2	23.2	8.6
0.27	14.8	25.3	30.1	17.1	20.1	4.2
0.28	13.5	20.1	25.7	25.4	17.3	5.1
0.38	23.1	15.1	48.3	40.3	31.5	12.4
0.43	14.8	17.1	66.5	25.6	30.8	9.5
0.46	21.4	7.5	91.2	40.1	38.2	9.3
0.51	27.1	16.2	96.3	63.2	44.5	9.5
0.59	25.8	20.3	72.5	55.7	44.6	20.1
0.63	18.7	10.4	90.2	63.1	59.2	20.3
0.69	24.2	26.2	89.4	62.5	57.1	22.1
0.73	23.5	46.3	99.8	46.7	44.2	28.3
0.78	25.1	79.5	99.5	50.2	57.2	22.1
0.82	48.9	70.3	47.6	60.3	49.3	37.2

In the first parts of μ-v curves (sliding speed up to 0.28 m/s), the ranges of the coefficient of friction overlapped for specimens with pit-area ratios of 10%, 15%, and the non-textured block. In this case, the coefficient of friction was higher in comparison to other sliding pairs. For higher speeds, the values of μ coefficient of assemblies with the smallest pit-area ratio (of 4 and 6.5%) of the block sample were significantly smaller than those of the other cases. The values of the coefficient of friction continuously decreased from about 0.1 to values smaller than 0.02. The shapes of the other curves corresponding to textured samples were different. The highest value of the coefficient of friction was obtained for the non-textured block sample. However, in this case, the values of coefficient of friction overlapped with those corresponding to the specimen with an area

density of 15%. The ranges of the μ coefficient of sliding pairs with samples of S_p = 10% and 20%, and they did not overlap when the sliding speed was higher than 0.66 m/s. It is interesting that the relative scatter of the coefficient of friction was higher for the higher sliding speed. However, the values of the coefficient of friction of samples with the smallest area density of dimples (S_p = 4%, 6.5%) were significantly smaller than those of other sliding pairs despite large values of the relative scatter. In these cases, oil temperature was also the lowest; therefore, the maximum value of the λ parameter was the highest (see **Figure 4**).

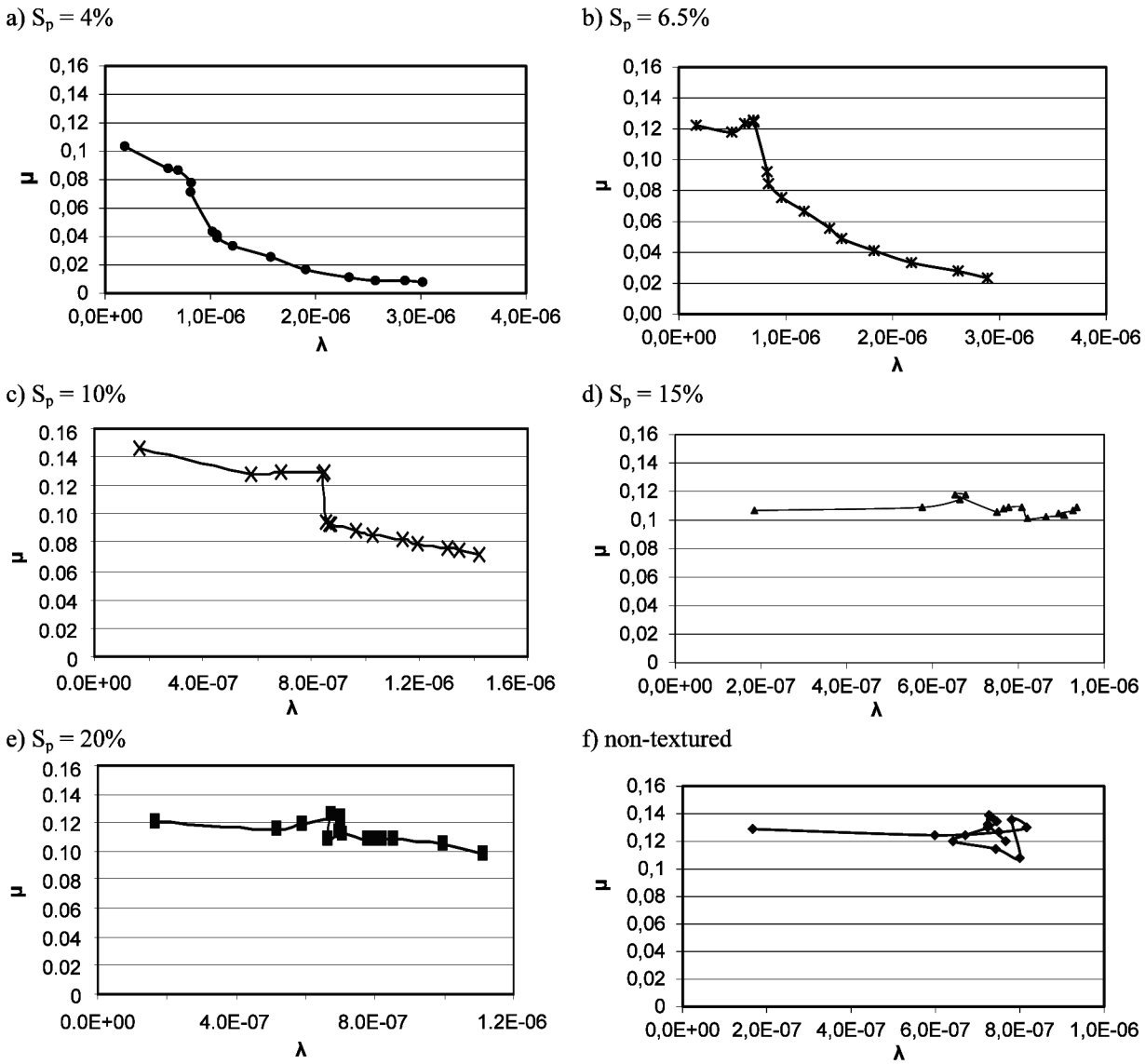

Fig. 4. Coefficient of friction μ versus the λ parameter for assemblies with textured and non-textured surface
Rys. 4. Współczynnik tarcia μ w funkcji parametru λ dla skojarzeń zawierających powierzchnie teksturowane i nieteksturowane

The changes in the friction force for sliding speed increase may be correlated with changes in oil temperature. Oil temperature in all the cases initially decreased, reached a minimum value for a speed of 0.27 m/s (46–49°C), then increased continuously for samples with the largest pit-area ratio (15 and 20%); however, for the other samples (of smaller pit-area ratio), changes in oil temperature were different, i.e. the temperature reached the maximum value for the sliding speed of 0.46 m/s and then decreased. Generally, lower oil temperatures corresponded to smaller coefficients of friction.

The frictional behaviour of the sliding pair with non-textured block sample was the worst. In this case, the maximum temperature of the lubricating oil was also the highest – about 90°C. The final coefficient of friction was 0.16.

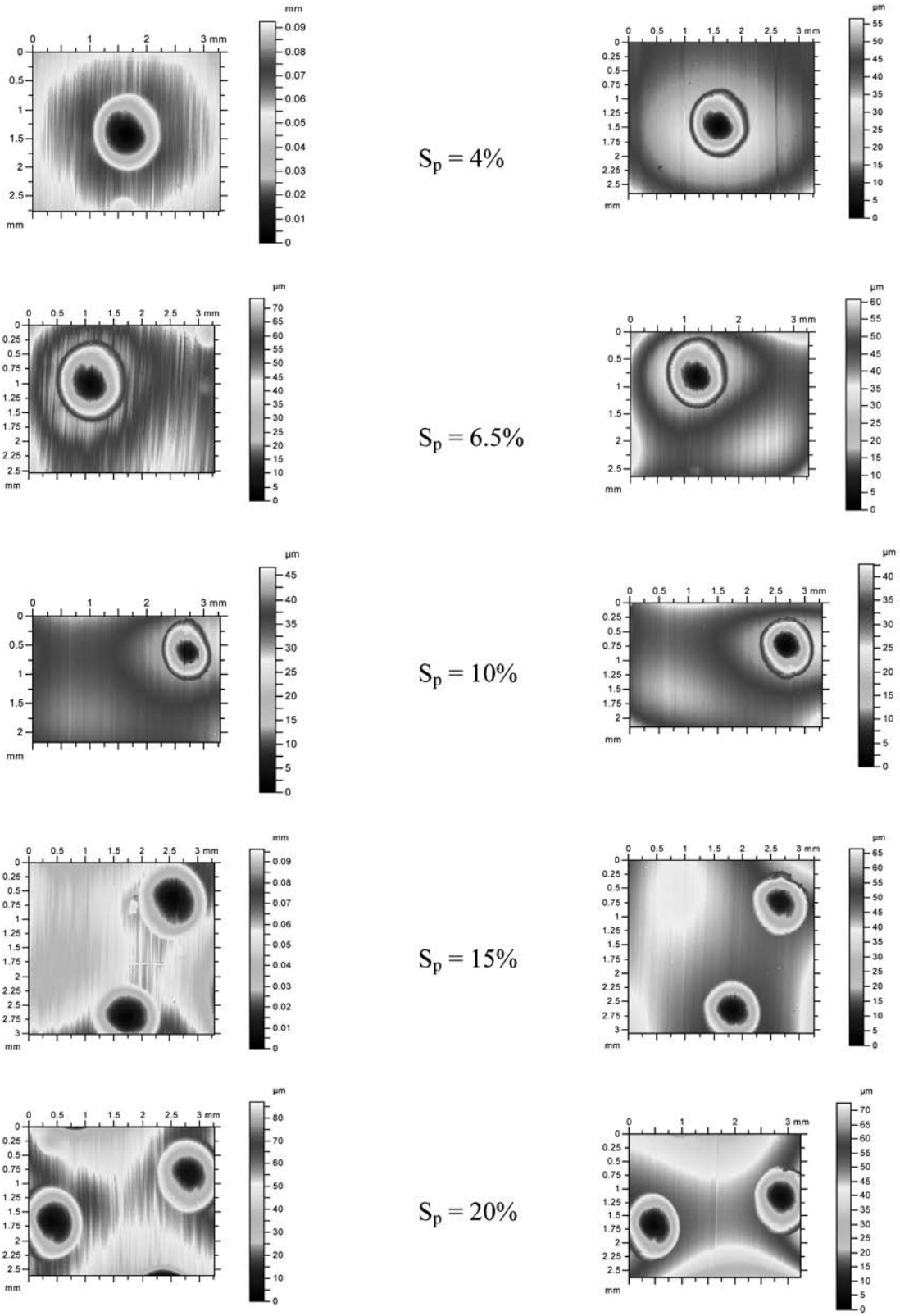

Fig. 5. Contour plots of textured block samples before (left) and after friction (right)
Rys. 5. Mapy powierzchni próbek teksturowanych przed (z lewej) oraz po badaniach (z prawej)

The resistance to motion was also high for samples with a pit-area ratio of 20% and especially 15%. In those cases, only mixed lubrication took place. The beneficial effect of surface texturing was visible mainly for block samples with the smallest area density of oil pockets – 4% and 6.5%. For a sliding speed of 0.82 m/s, surface

texturing caused a decrease in the friction force of more than 8 times compared to the non-textured sample. The advantageous effect of surface texturing on fictional resistance was also found for the sample with S_p =10%. The non-beneficial effect of surface texturing with a high area density of dimples can be explained by the decrease of load carrying capacity due to the increase of unitary pressure. Due to the presence of dimples, hydrodynamic lift formation was possible for low density areas of oil pockets. In abrasive wear resistance tests, the wear of the textured block sample with S_p = 4% was the smallest **[L. 10]**.

The study of changes in surface topography parameters during friction is an additional source of information about this process. It was found that depths of oil pockets decreased between 2 μm and 15 μm. The tendency was found that a larger change (higher wear) corresponded to a higher friction force. When the decrease in dimples depth was smaller, changes in surface topography parameters were also lower. All height parameters decreased; the changes in statistical parameters Sa (arithmetical mean deviation of the surface height), Sq (root-mean square deviation of the surface height) and total height of the surface Sz were smaller than 30%. Changes in the maximum height of valleys Sv were smaller (up to 16%) but with the maximum height of peaks higher (to 70%) due to the wear of only the peak parts of surfaces. The skewness Ssk decreased, and the kurtosis Sku decreased, which is typical to changes for a low wear process **[L. 8]**. Because surface height and skewness Ssk decreased as well as kurtosis, one can conclude that, during the friction process, mainly wear removal took place. Usually, peak density Spd and spatial parameters like fastest decay autocorrelation length Sal and texture aspect ratio of the surface Str decreased during frictional process. The parameters describing hybrid properties as rms. slope Sdq, developed interfacial area ratio Sdr, and mean peak curvature Spc decreased during wear. Their changes, which are comparatively high (decreases in the Sdr parameter were sometimes larger than 90%), are mainly the results of surface height decrease and, to a smaller degree, the decrease in spatial parameter Sal. The main surface texture direction Std was constant during the friction process due to small changes in the dementions of the oil pockets (dimples lay-out mainly affected this parameter value). **Figure 5** shows contour plots of textured block surfaces before and after friction tests. Decreases in the total surface heights were mainly caused by the reductions of dimple depths due to wear.

The study of changes in surface topography in areas free from oil pockets can give us additional information about the character of wear. The surface becomes smoother as a result of friction processes. The relative decreases in surface parameters characterizing amplitude were comparatively high (sometimes larger than 90%). Surface texture oriented parallel to the direction of ring motion was formed in the tribologic process.

CONCLUSIONS

The dimple presence on the bronze surface was observed to reduce the friction coefficient substantially, when compared with non-textured surfaces (after turning). It appears that the dimple density smaller than 15% is beneficial. The best behaviour with regard to minimizing the friction force was observed for samples with pit-area ratios Sp = 4% and Sp = 6.5%. When sliding speed was about 0.8 m/s, the friction force of frictional pairs with these samples was more than 8 times lower than that with non-textured specimen. The lower oil temperatures corresponded to lower coefficients of friction.

During friction, the peaks of surface topography containing dimples changed. The tendency was found that higher decreases in dimples depths corresponded to higher friction forces. In areas without oil pockets, surface topography oriented parallel to direction of ring motion was created in the friction process with much smaller heights than that after machining.

REFERENCES

1. Mezghani S., Demirci I., Yousfi M., El Mansori M.: Mutual influence of crosshatch angle and superficial roughness of honed surfaces on friction in ring-pack tribo-system, Tribology International 66 (2013), pp. 54–59.
2. Tomanik E., El Mansori M., Souza R., Profito F.: Effect of waviness and roughness on cylinder liner friction, Tribology International 120 (2018), pp. 547–555.
3. Wos S., Koszela W., Pawlus P., Drabik J., Rogos E.: Effects of surface texturing and kind of lubricant on the coefficient of friction at ambient and elevated temperatures, Tribology International 117 (2018), pp. 174–179.
4. Wos S., Koszela W., Pawlus P.: The effect of both surfaces textured on improvement of tribological properties of sliding elements, Tribology International 113 (2017), pp. 182–188.
5. Vlădescu S-C., Medina S., Olver A.V., Pegg I.G., Reddyhoff T.: Lubricant film thickness and friction force measurements in a laser surface textured reciprocating line contact simulating the piston ring–liner pairing, Tribology International 98 (2016), pp. 317–329.

6. Etsion I.: State of the art in laser surface texturing. In: Proceedings of the 12th International Conference on Metrology and Properties of Engineering Surfaces, Rzeszow, Poland, (2009), pp. 17–20.
7. Gałda L., Pawlus P., Sęp J.: Dimples shape and distribution effect on characteristics of Stribeck curve. Tribology International 42 (2009), pp. 1505–1512.
8. Koszela W., Dzierwa A., Gałda L., Pawlus P.: Experimental investigation of oil pockets effect on abrasive wear resistance. Tribology International 46 (2012), pp. 145–153.
9. Nilsson B., Rosen B.-G., Thomas T.R., Wiklund D., Xiao L.: Oil pockets and surface topography: mechanism of friction reduction. In: XI International Colloquium on Surfaces, Chemnitz, Germany, Addendum (2004).
10. Gachot C., Rosenkranz A., Hsu SM.**,** Costa HL.: A critical assessment of surface texturing for friction and wear improvement, Wear 372–373 (2017), pp. 21–41.
11. Loring S.H., Brown R.E., Gouldstone A., Butler J.P.: Lubrication regimes in mesothelial sliding. Journal of Biomechanics 38 (2005), pp. 2390–2396.
12. Lee S.Y., Kim S.D., Hong Y.S.: Application of the duplex TiN coatings to improve the tribological properties of electro hydrostatic actuator pump parts. Surface and Coatings Technology 193 (2005), pp. 266–271.
13. Kovalchenko A., Ajayi O., Erdemir A., Fenske G., Etsion I.: The effect of laser surface texturing on transitions in lubrication regimes during unidirectional sliding contact. Tribology International 38 (2005), pp. 219–225.
14. Wang X., Kato K., Adachi K., Aizawa K.: The effect of laser texturing of SiC surface on the critical load for the transition from water lubrication mode from hydrodynamic to mixed. Tribology International 34 (2001), pp. 703–711.
15. Wang X., Kato K., Adachi K., Aizawa K.: Load carrying capacity map for the surface design of SiC thrust bearing sliding in water. Tribology International 36 (2003), pp. 189–197.
16. Lu X., Khonsari M.M.: An experimental investigation of dimple effect on the Stribeck curve of journal bearings. Tribology Letters 27 (2007), pp. 169–176.
17. Blunt L., Jiang X. (eds): Advanced techniques for assessment surface topography. Kogan Page Science, London and Sterling (2003).
18. So H., Chen C.H.: Effects of micro-wedges formed between parallel surfaces on mixed lubrication – Part I: Experimental evidence. Tribology Letters 17/3 (2004), pp. 513–520.